JOURNAL OF CHEMICAL INFORMATION AND MODELING

Letter

pubs.acs.org/jcim

# Repurposing Registered Drugs as Antagonists for Protease-Activated Receptor 2

Weijun Xu,[†] Junxian Lim,[†] Chai-Yeen Goh, Jacky Y. Suen, Yuhong Jiang, Mei-Kwan Yau, Kai-Chen Wu, Ligong Liu, and David P. Fairlie*

Division of Chemistry and Structural Biology, Institute for Molecular Bioscience, The University of Queensland, Brisbane, Queensland 4072, Australia

Supporting Information

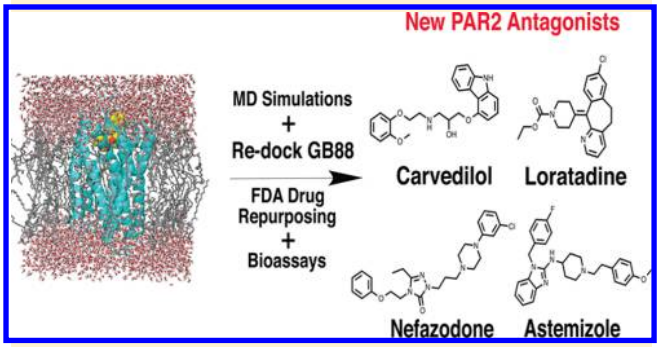


**ABSTRACT:** Virtual screening of a drug database identified Carvedilol, Loratadine, Nefazodone and Astemizole as PAR2 antagonists, after ligand docking and molecular dynamics simulations using a PAR2 homology model and a putative binding mode of a known PAR2 ligand. The drugs demonstrated competitive binding and antagonism of calcium mobilization and ERK1/2 phosphorylation in CHO-hPAR2 transfected cells, while inhibiting IL-6 secretion in PAR2 expressing MDA-MB-231 breast cancer cells. This research highlights opportunities for GPCR hit-finding from FDA-approved drugs.

## INTRODUCTION

Drug discovery via traditional high-throughput compound screening usually furnishes small molecule ligands with modest affinities at low hit rates, with considerable subsequent efforts needed for hit-to-lead development and adequate profiling for selectivity, toxicity, pharmacokinetics, pharmacodynamics, and formulation/delivery. In the past decade, only 0.01% of new drug leads were selected for clinical trials,[1] representing a poor return on medicinal chemistry investment. An alternative approach gaining favor in drug discovery is the repurposing of FDA-approved drugs for new uses, facilitating faster and cheaper progression to the clinic.[2] There have been several examples of successful drug repurposing,[3−5] and there are many examples of drugs approved by the U.S. Food and Drug Administration that show promising activities against multiple targets.[6]

Protease-activated receptor 2 (PAR2) is a unique GPCR where there is no known endogenous ligand. Instead, PAR2 is activated by proteases.[7−9] Its extracellular N-terminus is cleaved predominately by trypsin-like serine proteases to reveal a "neoepitope" called the tethered ligand (TL), (e.g., SLIGKV, human; SLIGRL, murine), which binds intramolecularly and activates PAR2 at an unknown site.[10,11] Studies have shown that PAR2 activation is associated with metabolism, inflammation, pain, proliferation, metastasis, angiogenesis, and many cancers including pancreatic, colon, breast, prostate and stomach.[12] Modulation of PAR2 represents a potential therapeutic strategy for treating many diseases. Our group developed small, serum stable, nonpeptidic agonists (e.g., GB110, $EC_{50}$ ∼ 200 nM, $Ca^{2+}$, HT29 cells)[13] and antagonists (e.g., GB88, $IC_{50}$ 1−10 $\mu$M, $Ca^{2+}$)[14] that were effective in modulating PAR2 in a variety of human cell lines. GB88 has shown therapeutic benefits in both *in vitro* and *in vivo* models of diseases[15−17] and stimulated our interest in the development of small molecule modulators of human PAR2.

GPCRs are notorious for adopting multiple conformations, representing different active and inactive states that influence pharmacology. Studies have supported successful structural modeling of aminergic GPCRs, but historically there have been more difficulties in modeling the peptidergic GPCRs.[18] Several successful studies have reported virtual screening campaigns using homology structural models of GPCRs.[19] The number of studies seeking to repurpose drugs via computational approaches has steadily increased.[6] GPCRs in particular are often associated with multiple therapeutic areas, so GPCR ligands potentially represent good candidates for rational repurposing of drugs.[20]

Proof-of-principle is demonstrated here for the application of computer assisted molecular modeling, in combination with *in vitro* assays, to the mining of a database containing 1216 FDA-approved drugs for modulating the function of a GPCR known as PAR2. From 150 virtual hits, 8 were selected for bioassay and 4 of these were inhibitors of PAR2, a hit rate that should encourage future applications of the methodology to other GPCRs.

## RESULTS AND DISCUSSION

Previously, we used homology models of human PAR2, based on the template crystal structure of human nociceptin opioid receptor (ORL-1), to identify putative binding modes of PAR2 agonists and to pan for PAR2 antagonists through virtual screening of a commercial database (Chembridge).[21] In this study, we instead began with putative binding modes of the PAR2 antagonist GB88[14] and identified an ensemble of

Published: October 7, 2015





DOI: 10.1021/acs.jcim.5b00500
J. Chem. Inf. Model. 2015, 55, 2079−2084

molecular dynamics (MD) snapshot poses of the docked ligand in the PAR2 homology model. Representative conformations were sampled and used for prospective docking of various FDA-approved drugs (Figure 1).

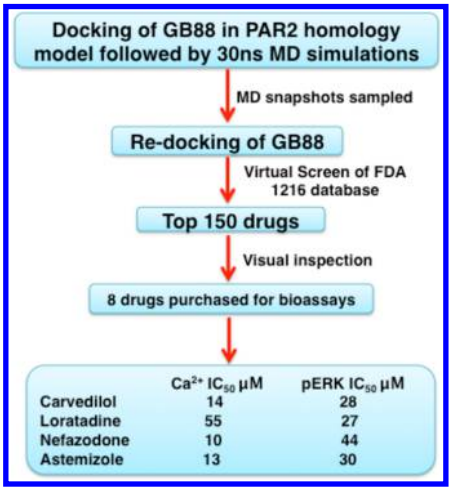


**Figure 1.** Modeling and virtual screening approach to novel scaffold discovery for PAR2.

Figure 2A shows a superimposed structure of the homology model of PAR2 with the template ORL-1 crystal structure

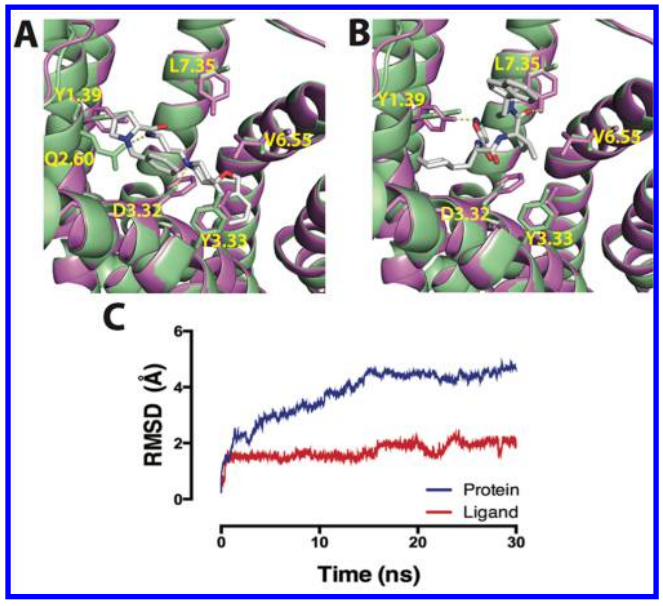


**Figure 2.** Superposition of the PAR2 homology model with the crystal structure of the template structure. (A) PAR2 homology model (violet) vs crystal structure of ORL-1 (green) (PDB code: 4EA3) bound to its antagonist C-24; (B) PAR2 homology model (violet) with GB88 docked and crystal structure of ORL-1 (green); (C) RMSD plot of protein (backbone) and ligand (heavy atoms) from MD simulations.

bound by its antagonist (C-24).[22] The original docking pose of the PAR2 ligand GB88 in the PAR2 homology model suggested that the isoxazole ring sits in a pocket near to TM1 and TM7 (Figure 2B). A potential hydrogen bond was predicted to form between Tyr82 (residue 1.39) and the nitrogen atom of isoxazole. Cyclohexylalanine (Cha) at the second position in GB88 binds between TM2 and TM3, near to Phe155 (3.32). Isoleucine at the third position in GB88 is near to Tyr156 (3.33), Leu307 (6.55), and the spiro[indene-1,4′-piperidine] of GB88 binds toward the surface of the TM near to Tyr326 (7.35). However, the exposure of the very hydrophobic spiroindenepiperidine to the solvent was inappropriate, and GB88 can likely adopt alternative poses not evidently sampled in the docking possibly because conformational flexibility of PAR2 was not a feature of the model.

On closer investigation of the template from which the model was built, the crystal structure of ORL-1 bound to antagonist C-24 led us to propose the possibility of other potential binding poses adopted by GB88. First, the right side of benzofuranpiperidine of C-24 is similar to the spiroindene-piperidine of the PAR2 ligand GB88. Because class A GPCRs often share a similar binding pocket and ligand location, the binding of the benzofuranpiperidine in a deeper pocket created by M3.36 and Y1.56 in ORL-1 might possibly be mimicked by the spiroindenepiperidine component of GB88 in PAR2. A more focused comparison among three residues of PAR2 and ORL-1 might explain why the spiroindenepiperidine in the docked pose of GB88 was not sampled in a similar pocket as queried. It was noticed that Asp3.32, Val6.55 and Leu7.35 in ORL-1 are replaced by three larger residues: Phe3.32, Leu6.55 and Tyr7.35 in PAR2. As shown in Figure 2B, the superposition of the crystal structure and homology model reveals a possible clash between the spiroindenepiperidine and the blocking phenyl side chain from Phe155 (3.32) in PAR2 during the molecular docking.

To explore other possible binding modes between PAR2 and GB88, a 30 ns MD simulation was performed on PAR2 docked with GB88 in a simulated POPC membrane environment. After MD simulations, a protein−ligand contact (Figure S1) was generated using the simulation event analysis function (Desmond System v3.5, D. E. Shaw Research, New York, NY, 2013). Results suggested that Tyr82 (1.39) could still make a direct H-bond or water-mediated interaction with isoxazole. Interestingly, another residue, K131 (2.60), not predicted by docking, emerged as the most frequent residue in contact with GB88 through direct hydrogen bonding with the second and third carbonyl oxygen of the ligand. Y1.39 has been reported as a well-conserved hotspot residue in other peptidergic GPCRs such as angiotensin and chemokine receptors.[23,24] In the CCR5 chemokine receptor structure[25] and the recently solved Angiotensin II receptor, antagonists interacted with Y1.39 via hydrogen bonds.[23] A similar protein−ligand interaction was also present in the opioid receptor structure,[22] in which Gln (2.60) formed a hydrogen bond to the antagonist.

Figure 2C shows the RMSD fluctuation of protein PAR2 and ligand GB88 throughout the simulation period. Stabilized by extensive protein−ligand interactions shown in Figure S1, the small molecule antagonist GB88 was not observed to adopt significant conformational changes compared to the protein, for which most flexibility was observed for the residues located in the intracellular loops. The ligand conformation was stable throughout the entire MD simulations, consistent with no tendency for the hydrophobic group to relocate into the alternative pocket mentioned above. The snapshots from MD simulations provided a new source of receptor conformations for further examination to explore other docking poses of GB88. Ensemble docking following structure relaxation has proven to be effective in the identification of several inhibitors for other proteins, which would not have been possible by


DOI: 10.1021/acs.jcim.5b00500
J. Chem. Inf. Model. 2015, 55, 2079−2084

docking into the original crystal structure only.[26,27] We integrated this concept into the present study. From MD snapshots, we surmised that sampling different structures of the receptor with different rotamers of F155 (3.32) might allow the proposed pocket to open up and create more space to accommodate the bulky spiroindenepiperidine of GB88. To test this hypothesis, structures of the receptor were sampled at 15, 20, 25 and 30 ns in MD simulations, with the aid of visual inspection for side-chain rotations of the above residues. Molecular docking of GB88 was performed again based on these sampled structures.

Encouragingly, it was found that in one of the sampled structures after 30 ns MD simulation, followed by docking of GB88 into the PAR2 structure, was the hypothesized binding mode of the antagonist (Figure S2). Indeed, the movement of the F3.32 side chain during MD simulations allowed the spiroindenepiperidine of GB88 to insert into the hydrophobic cage created by Y3.33 and F6.48. In other aminergic class A GPCRs, W6.48 was reported as a "toggle switch" residue that played an important role during receptor activation. PAR2 has a Phe at this topologically analogous position. The interaction between the spiroindenepiperidine of GB88 with this residue may be key to the mechanism of its antagonism of PAR2.

The finding of this docked pose of GB88 suggests a new possible inactive conformation of PAR2 for further ligand docking and modeling studies. Importantly, the hydrophobic interaction between the spiroindenepiperidine and the receptor aromatic cage residues (Y3.33, F6.48) may help differentiate biological profiles of PAR2 ligands. This has been reflected to some extent by SAR studies from our group, especially for small molecule potent agonists (unpublished), in which the C-terminal amide of the ligand putatively binds at an upper position without penetrating through the F155 mediated hydrophobic gate as compared to GB88 binding. The hydrophobic nature of GB88 might allow it to avoid F155 and hence penetrate even deeper into the pocket and, make hydrophobic interactions that lock the receptor in an inactive conformation.

A similar phenomenon has been observed in a crystal structure for the class B GPCR, the CRF receptor.[28] In that structure, antagonist binding is restricted by side chains of Phe 203 and Tyr 327 and for the ligand to reach the site it may require rearrangement of residues at the top of the site through side-chain rotamer changes and a shift of segments of TM3, TM5 and TM6, which then allows enlargement of the putative ligand-binding site. To validate the potential use of the discovered binding cavity adopted by GB88 as a novel site for prioritizing new PAR2 antagonists, we applied virtual ligand screening by docking 1216 FDA-approved drugs from the United States Environmental Protection Agency website (http://www.epa.gov/ncct/dsstox/sdf_fdamdd.html). Current scoring functions are generally capable of performing binding pose predictions from pose scoring, but are still not very efficient for predicting binding affinity even after ligands are docked into crystal structures of target proteins.[29,30] Consequently, the success rate of a virtual screening campaign also relies significantly on the experience and knowledge of the operator working with protein−ligand interactions and visual inspection can play an important role in determining the rate of success. The top ranking 150 drugs, as judged by ChemPLP scores from GOLD software, were further visually inspected for their docked poses and for interactions with residues in the putative binding site of PAR2. Thus, docking scores were used here as a first filter, to eliminate compounds unlikely to fit the putative docking site, and those with a relatively higher fitness score were retained for detailed visual inspection as a focused subset of the compound data set. Finally, 8 drugs were selected for bioassays based on the ranking list derived from virtual screening coupled with visual inspection of putative drug−receptor interactions.

Given the simulations and *in silico* docking data, we measured the PAR2-binding affinities of these 8 drugs (Figure S3) using CHO-hPAR2 cells and a competing europium(III)-labeled 2f-LIGRLO-dpta-$NH_2$ ligand for PAR2. Preliminary screening showed that Pimozide, Carvedilol, Loratadine, Nefazodone and Astemizole bound weakly to PAR2 at concentrations of 20−100 $\mu$M (Figure 3A). Concentration-dependent binding curves gave $IC_{50}$ values of 46, 28, 39, 24 and 16 $\mu$M, respectively (Figure 3B).

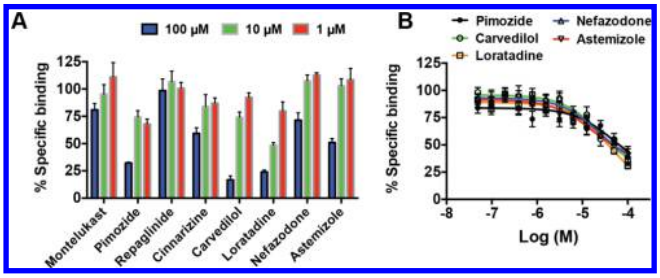


**Figure 3.** Competitive PAR2 binding affinity of FDA-registered drugs vs known agonist 2f-LIGRLO-dpta. (A) Ligand (3 concentrations) binding to CHO-hPAR2 cells. (B) Concentration−response curves for Pimozide, Carvedilol, Loratadine, Nefazodone and Astemizole in PAR2 binding assay. Data shown are means ± SEM of >3 independent experiments.

Functional antagonism by these drugs was determined using calcium mobilization, and 4 drugs (Carvedilol, Loratadine, Nefazodone, Astemizole) were found to have ≥50% inhibition at 30 $\mu$M (Figure 4A). These compounds were chosen for further concentration−response measurements, with $IC_{50}$ = 14, 55, 10 and 13 $\mu$M, respectively (Figure 4B). Pimozide was not a PAR2 antagonist in the $Ca^{2+}$ release assay. To ensure that the antagonism of the four drugs was not due to their agonist-induced desensitization of PAR2, the agonist activity of each drug alone was also measured (Figure S4). The PAR2 ligands exhibited minimal agonist activity (Figure S4). Together, the binding and $Ca^{2+}$ mobilization results suggested that the four drugs inhibited PAR2 activation via docking in a similar binding site as the agonist 2f-LIGRLO-$NH_2$ in PAR2.

Carvedilol, Loratadine, Nefazodone and Astemizole were also tested for antagonism of PAR2-mediated ERK1/2 phosphorylation, a well-documented reporter of a different GPCR signaling pathway that has been linked to cancer development and inflammatory diseases.[31] Consistent with the $Ca^{2+}$ mobilization data, Carvedilol ($IC_{50}$ = 28 $\mu$M), Loratadine ($IC_{50}$ = 27 $\mu$M), Nefazodone ($IC_{50}$ = 44 $\mu$M) and Astemizole ($IC_{50}$ = 30 $\mu$M) all inhibited PAR2-mediated ERK1/2 phosphorylation (Figure 4C) without detectable agonist properties. The finding of inhibition of ERK1/2 phosphorylation by four PAR2 antagonists is noteworthy, since most PAR2 antagonists reportedly inhibit calcium mobilization but not ERK1/2 phosphorylation, one exception[32] being C391, which is an analogue of the agonist 2f-LIGRLO-$NH_2$.


DOI: 10.1021/acs.jcim.5b00500
J. Chem. Inf. Model. 2015, 55, 2079−2084

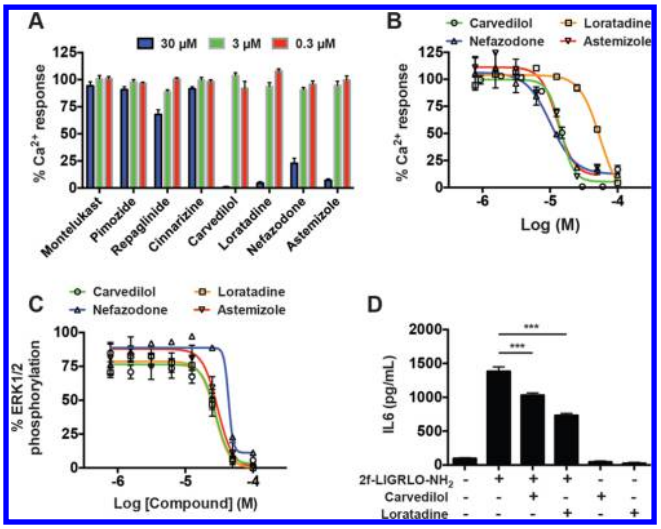


**Figure 4.** FDA-registered drugs are PAR2 antagonists. (A) Antagonism of calcium mobilization in CHO-hPAR2 cells by FDA-approved drugs. (B) Concentration-dependent inhibition of PAR2-mediated calcium mobilization. (C) Concentration-dependent inhibition of PAR2-mediated ERK1/2 phosphorylation (D) Carvedilol or loratadine (30 $\mu$M) inhibited PAR2-mediated IL-6 secretion from MDA-MB-231 human breast cancer cells. Data shown are means ± SEM of >3 independent experiments. ***$P$ < 0.001; significant differences as indicated.

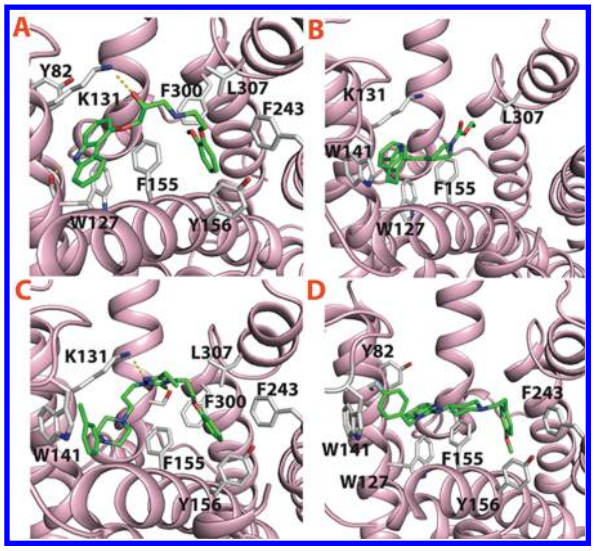


**Figure 5.** Molecular docking poses of four drugs within the PAR2 homology model after 30 ns of molecular dynamics simulations. (A) Carvedilol (R-enantiomer docked here), (B) Loratadine, (C) Nefazodone and (D) Astemizole.

Because PAR2 is a mediator of inflammation and cancer,[33,34] the four antagonists were also investigated for inhibition of PAR2-mediated IL-6 secretion in human MDA-MB-231 breast cancer cells. Both Loratadine and Carvedilol (30 $\mu$M) blocked PAR2-mediated secretion of the inflammatory cytokine IL-6 in these cells (Figure 4D). IL-6 has been linked to inflammatory diseases and cancers[35] and is involved in the recruitment and activation of JNK and downstream activation of cell proliferation and differentiation.[36] In cancer, IL-6 decreases cancer cell apoptosis, promotes angiogenesis and therapy resistance, and IL-6 serum levels correlate with the clinical stage of breast cancer and prognosis.[37] Loratadine and Carvedilol may be useful scaffolds for building PAR2 antagonists into anticancer agents.

To identify putative binding modes of the drugs in PAR2, molecular docking with more GA runs (30 for each ligand) was performed in the binding site used for the virtual screening. Docking simulations predicted binding sites of these drugs to be the same as for GB88 (Figure 5). For Carvedilol (Figures 5A and S5A), the tricyclic carbazole ring was sandwiched by Y82 and W127, the hydrogen atom on the ring forms a hydrogen bond with the carbonyl oxygen of W127, the hydroxyl group forms a putative hydrogen bond with K131, while the 2-methoxyphenoxy group docks within the hydrophobic cleft mentioned above. Loratadine, being a smaller molecule compared to the others, partially binds in the pocket occupied by the other drugs (Figures 5B and S5B). The lack of interaction with the hydrophobic cleft residues may explain its weaker activity compared to the other drugs. Nefazodone (Figures 5C and S5C) and Astemizole (Figures 5D and S5D) adopted similar binding poses as Carvedilol, interacting with similar residues in the same binding pocket. An interesting observation is that all drug hits identified here originally targeted the aminergic group of class A GPCRs (e.g., Carvedilol for $\beta$1 adrenoreceptor, Loratadine and Astemizole for histamine H1-receptor, Nefazodone for $5HT_{1A}$). Therefore, a focused comparison of the ligand accessible binding site in PAR2 with these other receptors was also performed using the GPCRDB web tool (http://tools.gpcr.org/).[38] Figure S6 summarizes residue similarities and differences at the ligand-binding site of these receptors. Hydrophobic residues dominated the binding site similarity among the 4 GPCRs, whereas the major difference observed was for conserved polar residues in the aminergic family (e.g., D3.32, T3.37, S5.42, S5.46 in $\beta$1 adrenoreceptor). Such differences in the binding site prevent the drugs form forming key hydrogen bond contacts with the hydrophobic residues at the corresponding conserved position in PAR2 (e.g., F3.32, Y3.37, L5.42, V5.46 in PAR2). This is consistent with the predicted interactions from docking, involving mainly hydrophobic interactions of the drugs with the receptor, which resulted in only weak antagonism of PAR2. Nonetheless, these hits, together with their predicted binding modes, may help guide further hit-to-lead development.

In conclusion, this research began by predicting a putative binding site for a PAR2 antagonist (GB88) and then used this to conduct virtual screening of FDA-approved drugs for potential antagonism of PAR2. The predicted binding site, refined by molecular dynamics simulations, resulted in a promising high hit rate in the virtual screen. Computational simulations helped guide selection and optimization of the protein conformation bound to a known antagonist, which in turn aided the identification of the FDA-approved drugs (Nefazodone, Astemizole, Carvedilol, Loratadine) as novel PAR2 antagonists (Table S1), the latter two inhibiting PAR2-mediated IL-6 secretion in MDA-MB-231 human breast cancer cells. This approach to finding scaffolds for drug development might be useful in other cases where a receptor crystal structure is similarly not available. MD simulations have gained in popularity recently as part of the arsenal of computational tools developed to explore the design of novel bioactive molecules and for investigating the mode of actions of ligands on their protein targets.[39] These findings have demonstrated the potential of virtual screening of FDA-approved drugs to find


DOI: 10.1021/acs.jcim.5b00500
J. Chem. Inf. Model. 2015, 55, 2079−2084

novel hits that may be useful new scaffolds for hit-to-lead development and repurposing against alternative drug targets.

## ■ ASSOCIATED CONTENT

### Supporting Information

The Supporting Information is available free of charge on the ACS Publications website at DOI: 10.1021/acs.jcim.5b00500.

Protein−ligand contacts plot between PAR2 and GB88 throughout 30 ns MD simulations is shown in Figure S1. Redocked pose of GB88 into PAR2 homology model, the conformation sampled at 30 ns post-MD simulations is illustrated in Figure S2. Structures of 8 FDA-approved drugs are shown in Figure S3. Agonist activity of 4 drugs in calcium mobilization in CHO-hPAR2 cells is shown in Figure S4. 2D protein−ligand interaction plots for the drug hits are shown in Figure S5. Focused comparison at the ligand accessible binding site of PAR2 against three class A GPCRs is shown in Figure S6. Table S1 summarizes FDA-approved drugs used in this study. All experimental details are described under the Methods section herein (PDF).

## ■ AUTHOR INFORMATION


### Corresponding Author

*Professor David Fairlie. Fax: 61733462990. E-mail: d.fairlie@imb.uq.edu.au.

### Author Contributions

†These authors contributed equally to this work.


### Notes

The authors declare no competing financial interest.

## ■ ACKNOWLEDGMENTS

We acknowledge the Australian Research Council for a grant (DP130100629) and for a Centre of Excellence in Advanced Molecular Imaging grant (CE140100011); the National Health and Medical Research Council for grants (1084083, 1047759) and a Senior Principal Research Fellowship to D.F. (1027369), and the Qld Government for a CIF grant.

## ■ REFERENCES


(1) Milardi, D.; Pappalardo, M. Molecular Dynamics: New Advances in Drug Discovery. *Eur. J. Med. Chem.* **2015**, *91*, 1−3.

(2) Jin, G.; Wong, S. T. Toward Better Drug Repositioning: Prioritizing and Integrating Existing Methods into Efficient Pipelines. *Drug Discovery Today* **2014**, *19*, 637−644.

(3) Ashburn, T. T.; Thor, K. B. Drug Repositioning: Identifying and Developing New Uses for Existing Drugs. *Nat. Rev. Drug Discovery* **2004**, *3*, 673−683.

(4) Najm, F. J.; Madhavan, M.; Zaremba, A.; Shick, E.; Karl, R. T.; Factor, D. C.; Miller, T. E.; Nevin, Z. S.; Kantor, C.; Sargent, A.; Quick, K. L.; Schlatzer, D. M.; Tang, H.; Papoian, R.; Brimacombe, K. R.; Shen, M.; Boxer, M. B.; Jadhav, A.; Robinson, A. P.; Podojil, J. R.; Miller, S. D.; Miller, R. H.; Tesar, P. J. Drug-Based Modulation of Endogenous Stem Cells Promotes Functional Remyelination. *Nature* **2015**, *522*, 216−220.

(5) Fowler, B. J.; Gelfand, B. D.; Kim, Y.; Kerur, N.; Tarallo, V.; Hirano, Y.; Amarnath, S.; Fowler, D. H.; Radwan, M.; Young, M. T.; Pittman, K.; Kubes, P.; Agarwal, H. K.; Parang, K.; Hinton, D. R.; Bastos-Carvalho, A.; Li, S.; Yasuma, T.; Mizutani, T.; Yasuma, R.; Wright, C.; Ambati, J. Nucleoside Reverse Transcriptase Inhibitors Possess Intrinsic Anti-Inflammatory Activity. *Science* **2014**, *346*, 1000−1003.

(6) Ekins, S.; Williams, A. J.; Krasowski, M. D.; Freundlich, J. S. *In Silico* Repositioning of Approved Drugs for Rare and Neglected Diseases. *Drug Discovery Today* **2011**, *16*, 298−310.

(7) Ramachandran, R.; Noorbakhsh, F.; Defea, K.; Hollenberg, M. D. Targeting Proteinase-Activated Receptors: Therapeutic Potential and Challenges. *Nat. Rev. Drug Discovery* **2012**, *11*, 69−86.

(8) Zhao, P.; Lieu, T.; Barlow, N.; Metcalf, M.; Veldhuis, N. A.; Jensen, D. D.; Kocan, M.; Sostegni, S.; Haerteis, S.; Baraznenok, V.; Henderson, I.; Lindstrom, E.; Guerrero-Alba, R.; Valdez-Morales, E. E.; Liedtke, W.; McIntyre, P.; Vanner, S. J.; Korbmacher, C.; Bunnett, N. W. Cathepsin S Causes Inflammatory Pain Via Biased Agonism of PAR2 and TRPV4. *J. Biol. Chem.* **2014**, *289*, 27215−27234.

(9) Zhao, P.; Lieu, T.; Barlow, N.; Sostegni, S.; Haerteis, S.; Korbmacher, C.; Liedtke, W.; Jimenez-Vargas, N. N.; Vanner, S. J.; Bunnett, N. W. Neutrophil Elastase Activates PAR2 and TRPV4 to Cause Inflammation and Pain. *J. Biol. Chem.* **2015**, *290*, 13875−13887.

(10) Nystedt, S.; Emilsson, K.; Larsson, A. K.; Strombeck, B.; Sundelin, J. Molecular Cloning and Functional Expression of the Gene Encoding the Human Proteinase-Activated Receptor 2. *Eur. J. Biochem.* **1995**, *232*, 84−89.

(11) Vu, T. K.; Hung, D. T.; Wheaton, V. I.; Coughlin, S. R. Molecular Cloning of a Functional Thrombin Receptor Reveals a Novel Proteolytic Mechanism of Receptor Activation. *Cell* **1991**, *64*, 1057−1068.

(12) Yau, M. K.; Liu, L.; Fairlie, D. P. Toward Drugs for Protease-Activated Receptor 2 (PAR2). *J. Med. Chem.* **2013**, *56*, 7477−7497.

(13) Barry, G. D.; Suen, J. Y.; Le, G. T.; Cotterell, A.; Reid, R. C.; Fairlie, D. P. Novel Agonists and Antagonists for Human Protease Activated Receptor 2. *J. Med. Chem.* **2010**, *53*, 7428−7440.

(14) Suen, J. Y.; Barry, G. D.; Lohman, R. J.; Halili, M. A.; Cotterell, A. J.; Le, G. T.; Fairlie, D. P. Modulating Human Proteinase Activated Receptor 2 with a Novel Antagonist (GB88) and Agonist (GB110). *Br. J. Pharmacol.* **2012**, *165*, 1413−1423.

(15) Lohman, R. J.; Cotterell, A. J.; Barry, G. D.; Liu, L.; Suen, J. Y.; Vesey, D. A.; Fairlie, D. P. An Antagonist of Human Protease Activated Receptor-2 Attenuates PAR2 Signaling, Macrophage Activation, Mast Cell Degranulation, and Collagen-Induced Arthritis in Rats. *FASEB J.* **2012**, *26*, 2877−2887.

(16) Lohman, R. J.; Cotterell, A. J.; Suen, J.; Liu, L.; Do, A. T.; Vesey, D. A.; Fairlie, D. P. Antagonism of Protease-Activated Receptor 2 Protects against Experimental Colitis. *J. Pharmacol. Exp. Ther.* **2012**, *340*, 256−265.

(17) Suen, J. Y.; Cotterell, A.; Lohman, R. J.; Lim, J.; Han, A.; Yau, M. K.; Liu, L.; Cooper, M. A.; Vesey, D. A.; Fairlie, D. P. Pathway-Selective Antagonism of Proteinase Activated Receptor 2. *Br. J. Pharmacol.* **2014**, *171*, 4112−4124.

(18) Tarcsay, A.; Paragi, G.; Vass, M.; Jojart, B.; Bogar, F.; Keseru, G. M. The Impact of Molecular Dynamics Sampling on the Performance of Virtual Screening against GPCRs. *J. Chem. Inf. Model.* **2013**, *53*, 2990−2999.

(19) Thomas, T.; McLean, K. C.; McRobb, F. M.; Manallack, D. T.; Chalmers, D. K.; Yuriev, E. Homology Modeling of Human Muscarinic Acetylcholine Receptors. *J. Chem. Inf. Model.* **2014**, *54*, 243−253.

(20) Anighoro, A.; Bajorath, J.; Rastelli, G. Polypharmacology: Challenges and Opportunities in Drug Discovery. *J. Med. Chem.* **2014**, *57*, 7874−7887.

(21) Perry, S. R.; Xu, W.; Wirija, A.; Lim, J.; Yau, M. K.; Stoermer, M. J.; Lucke, A. J.; Fairlie, D. P. Three Homology Models of PAR2 Derived from Different Templates: Application to Antagonist Discovery. *J. Chem. Inf. Model.* **2015**, *55*, 1181−1191.

(22) Thompson, A. A.; Liu, W.; Chun, E.; Katritch, V.; Wu, H.; Vardy, E.; Huang, X. P.; Trapella, C.; Guerrini, R.; Calo, G.; Roth, B. L.; Cherezov, V.; Stevens, R. C. Structure of the Nociceptin/Orphanin FQ Receptor in Complex with a Peptide Mimetic. *Nature* **2012**, *485*, 395−399.

(23) Zhang, H.; Unal, H.; Gati, C.; Han, G. W.; Liu, W.; Zatsepin, N. A.; James, D.; Wang, D.; Nelson, G.; Weierstall, U.; Sawaya, M. R.; Xu, Q.; Messerschmidt, M.; Williams, G. J.; Boutet, S.; Yefanov, O. M.;




DOI: 10.1021/acs.jcim.5b00500
*J. Chem. Inf. Model.* 2015, 55, 2079−2084

White, T. A.; Wang, C.; Ishchenko, A.; Tirupula, K. C.; Desnoyer, R.; Coe, J.; Conrad, C. E.; Fromme, P.; Stevens, R. C.; Katritch, V.; Karnik, S. S.; Cherezov, V. Structure of the Angiotensin Receptor Revealed by Serial Femtosecond Crystallography. *Cell* **2015**, *161*, 833−844.
(24) Burg, J. S.; Ingram, J. R.; Venkatakrishnan, A. J.; Jude, K. M.; Dukkipati, A.; Feinberg, E. N.; Angelini, A.; Waghray, D.; Dror, R. O.; Ploegh, H. L.; Garcia, K. C. Structural Biology. Structural Basis for Chemokine Recognition and Activation of a Viral G Protein-Coupled Receptor. *Science* **2015**, *347*, 1113−1117.
(25) Tan, Q.; Zhu, Y.; Li, J.; Chen, Z.; Han, G. W.; Kufareva, I.; Li, T.; Ma, L.; Fenalti, G.; Li, J.; Zhang, W.; Xie, X.; Yang, H.; Jiang, H.; Cherezov, V.; Liu, H.; Stevens, R. C.; Zhao, Q.; Wu, B. Structure of the CCR5 Chemokine Receptor-HIV Entry Inhibitor Maraviroc Complex. *Science* **2013**, *341*, 1387−1390.
(26) Chan, A. H.; Wereszczynski, J.; Amer, B. R.; Yi, S. W.; Jung, M. E.; McCammon, J. A.; Clubb, R. T. Discovery of *Staphylococcus Aureus* Sortase A Inhibitors Using Virtual Screening and the Relaxed Complex Scheme. *Chem. Biol. Drug Des.* **2013**, *82*, 418−428.
(27) Lexa, K. W.; Carlson, H. A. Protein Flexibility in Docking and Surface Mapping. *Q. Rev. Biophys.* **2012**, *45*, 301−343.
(28) Hollenstein, K.; Kean, J.; Bortolato, A.; Cheng, R. K.; Dore, A. S.; Jazayeri, A.; Cooke, R. M.; Weir, M.; Marshall, F. H. Structure of Class B GPCR Corticotropin-Releasing Factor Receptor 1. *Nature* **2013**, *499*, 438−443.
(29) Xu, W.; Lucke, A. J.; Fairlie, D. P. Comparing Sixteen Scoring Functions for Predicting Biological Activities of Ligands for Protein Targets. *J. Mol. Graphics Modell.* **2015**, *57*, 76−88.
(30) Damm-Ganamet, K. L.; Smith, R. D.; Dunbar, J. B., Jr.; Stuckey, J. A.; Carlson, H. A. CSAR Benchmark Exercise 2011−2012: Evaluation of Results from Docking and Relative Ranking of Blinded Congeneric Series. *J. Chem. Inf. Model.* **2013**, *53*, 1853−1870.
(31) Eishingdrelo, H.; Kongsamut, S. Minireview: Targeting GPCR Activated ERK Pathways for Drug Discovery. *Curr. Chem. Genomics Transl. Med.* **2013**, *7*, 9−15.
(32) Boitano, S.; Hoffman, J.; Flynn, A. N.; Asiedu, M. N.; Tillu, D. V.; Zhang, Z.; Sherwood, C. L.; Rivas, C. M.; DeFea, K.; Vagner, J.; Price, T. J. The Novel PAR2 Ligand C391 Blocks Multiple PAR2 Signaling Pathways *in Vitro* and *in Vivo*. *Br. J. Pharmacol.* **2015**, *172*, 4535−4545.
(33) Lim, J.; Iyer, A.; Liu, L.; Suen, J. Y.; Lohman, R. J.; Seow, V.; Yau, M. K.; Brown, L.; Fairlie, D. P. Diet-Induced Obesity, Adipose Inflammation, and Metabolic Dysfunction Correlating with PAR2 Expression Are Attenuated by PAR2 Antagonism. *FASEB J.* **2013**, *27*, 4757−4767.
(34) Su, S.; Li, Y.; Luo, Y.; Sheng, Y.; Su, Y.; Padia, R. N.; Pan, Z. K.; Dong, Z.; Huang, S. Proteinase-Activated Receptor 2 Expression in Breast Cancer and Its Role in Breast Cancer Cell Migration. *Oncogene* **2009**, *28*, 3047−3057.
(35) Calabrese, L. H.; Rose-John, S. Il-6 Biology: Implications for Clinical Targeting in Rheumatic Disease. *Nat. Rev. Rheumatol.* **2014**, *10*, 720−727.
(36) Snyder, M.; Huang, X. Y.; Zhang, J. J. Signal Transducers and Activators of Transcription 3 (STAT3) Directly Regulates Cytokine-Induced Fascin Expression and Is Required for Breast Cancer Cell Migration. *J. Biol. Chem.* **2011**, *286*, 38886−38893.
(37) Knupfer, H.; Preiss, R. Significance of Interleukin-6 (IL-6) in Breast Cancer (Review). *Breast Cancer Res. Treat.* **2007**, *102*, 129−135.
(38) Isberg, V.; Vroling, B.; van der Kant, R.; Li, K.; Vriend, G.; Gloriam, D. GPCRDB: An Information System for G Protein-Coupled Receptors. *Nucleic Acids Res.* **2014**, *42*, D422−425.
(39) Mortier, J.; Rakers, C.; Bermudez, M.; Murgueitio, M. S.; Riniker, S.; Wolber, G. The Impact of Molecular Dynamics on Drug Design: Applications for the Characterization of Ligand-Macromolecule Complexes. *Drug Discovery Today* **2015**, *20*, 686−702.


DOI: 10.1021/acs.jcim.5b00500
*J. Chem. Inf. Model.* 2015, 55, 2079−2084